International Journal of Applied and Natural Sciences (IJANS)
ISSN (P): 2319-4014; ISSN (E): 2319-4022
Vol. 7, Issue 1, Dec - Jan 2018; 7 - 16

International Academy of Science, Engineering and Technology
Connecting Researchers; Nurturing Innovations

INFLUENCE OF DENSITY-DEPENDENT COUPLING CONSTANTS, ON SYMMETRY ENERGY OF NUCLEAR MATTER

Xian-Mei Ye, Hua-Ju Lee & Wei Chen

Department of Physics, Jinan University, Guangzhou, China

ABSTRACT

In the mean field approximation of nonlinear relativistic $\sigma-\omega-\rho$ model, we study the influence of the density-dependent coupling constants, between nucleons and mesons on the symmetry energy $S(\rho_B)$ of infinite nuclear matter, in four different density-dependent formalism. We find greater Γ_ρ leads to greater K_{sym} and L when $\Gamma_{\sigma,\omega}$, c and d are fixed and indicate larger $S(\rho_B)$ in high density region. In addition, the density dependence of $\Gamma_{\sigma,\omega,\rho}$ make $S(\rho_B)$ smaller in high density region, and they make K_{sym} and L more sensitive to the changing of parameters at different density.

KEYWORDS: *Nuclear Matter, Density-Dependent Coupling Constants, Symmetry Energy*

CLC number: *O57*

Article History

Received: ***10 Nov 2017*** **|** ***Revised:*** ***16 Dec 2017*** **|** ***Accepted:*** ***04 Jan 2018***

1. INTRODUCTION

The nuclear symmetry energy, which is the difference of energy per nucleon between pure neutron matter and symmetric nuclear matter, characterizes the isospin dependent part of the equation of state (EOS), of asymmetric nuclear matter. The nuclear symmetry energy is closely related with the neutron skin of a nucleus and pressure of crust matter of neutron star, so it is an important topic in nuclear physics and astrophysics[1-4]. The information of the symmetry energy is especially interesting in related fields, and many theoretical and experimental efforts have been performed [5-7]. The $^3H/^3He$ ratio is sensitive to the nuclear symmetry energy at sub-saturation densities, within the newly updated version of the Ultra-relativistic quantum molecular dynamics (UrQMD) model[8]. The impact of the rearrangement term and momentum dependence of the single-particle potential, on the density dependence of the nuclear symmetry energy and nucleon effective mass has been studied in details [9]. Both the isospin-singlet and isospin-triplet components of the potential energy, play an important role, in determining the symmetry energy, when the Fock diagram is introduced within the covariant density functional (CDF) theory[10]. The findings reveal that, the ratio of relative yield of light charged particles poses better candidate, to probe the density dependence of nuclear symmetry energy, by using the yield of various fragments, in central collisions of various isotopic and isobaric colliding pairs [11]. The breakup reactions induced by the polarized deuteron beam at about 100 Mev/u, provide a more stringent constraint to the symmetry energy at sub saturation densities, via the calculations on a novel reorientation effect of deuteron attributed to is o vector interaction, in the nuclear field of heavy target nuclei [12]. An analytic expression for the symmetry energy as a function of its slope parameter L is found, by using a modified quark-meson coupling model [13]. A covariance analysis reveals that, the additional fitting protocol reduces the uncertainties in the nuclear symmetry energy coefficient, its slope parameter as well as the neutron-skin thickness in ^{208}Pb nucleus by 50%[14]. Assessments based on the sensitivity matrix reveal that, the properties of extreme neutron-rich systems play a predominant role, in narrowing down the uncertainties in the various symmetry energy parameters [15]. Four quantities deducible from nuclear structure experiments have been claimed to correlate to the slope parameter L of the symmetry energy [16]. Results from classical molecular dynamics simulations of infinite nuclear systems, show an excellent agreement with the experimental data and corroborate the claim that, the formation of clusters has a strong influence on the symmetry energy, in the liquid-gas coexistence region[17]. The slope of the symmetry energy plays an important role, in determining the boundary and properties of the mixed phase, in the study of the liquid-gas phase transition of stellar matter, with the inclusion of the finite-size effect from surface and Coulomb energies[18]. Some mean field models associated with similar values of L at saturation density, and pertaining to different families, yield a greater-than-expected spread, in the neutron-skin thickness of the ^{208}Pb nucleus[19]. And the main uncertainty of symmetry energy in finite nuclei is found to be related to the I^4 term, by investigating the model dependence of I^4 term in theoretical symmetry energy for a few popular mass models[20].

The recommended value of symmetry energy at saturation density is 31 MeV, and the behavior of symmetry energy below saturation density is now much better known, while the density above saturation is still not yet well constrained, and the predictions from different models strongly diverge. There are two different forms of the density dependence of the symmetry energy; the stiff dependence is the symmetry energy increases monotonically as the density increases, while the soft is the symmetry increases initially up to normal nuclear density and then decrease in higher density. It is essential to constrain the form of the density dependence of the symmetry energy for understanding the nucleon-nucleon interaction and the structure of the compact stellar objects such as the neutron star. The main reason of the uncertain symmetry energy is related to nuclear force and its spin and isospin dependence which have not been understood thoroughly.

The specific values of L and K_{sym} are model dependent, the ref. [21] gives $L = 46.7 \pm 12.8MeV$ and K_{sym} = -166.9 $\pm$ 168.3MeV, the studies on neutron skin[22] gain $L = 59 \pm 13.0MeV$, astrophysical observations of neutron star radii and masses[23] recommend $L = 48 \pm 4.0MeV$, while our conclusion on K_{sym} and L will be listed in Section 3 in detail.

In this paper, we study the influence of density-dependent coupling constants on symmetry energy of nuclear matter in the relativistic mean field (RMF) approximation of the relativistic $\sigma - \omega - \rho$ model. In Section 2 the mean field approximation of nonlinear relativistic $\sigma - \omega - \rho$ model and three density-dependent formulas of meson-nucleon coupling will be introduced.

In Section 3 the numerical results will be discussed in detail, and the paper closes in Section 4 with a summary and concluding remarks.

2. BASIC THEORIES

The Lagrange density in nonlinear relativistic $\sigma-\omega-\rho$ model is

$$\begin{aligned} L = & \sum_B \overline{\psi}_B (i\gamma_\mu \partial^\mu - m_B + \Gamma_\sigma \sigma - \Gamma_\omega \gamma_\mu \omega^\mu - \frac{1}{2}\Gamma_\rho \gamma_\mu \tau \cdot b^\mu)\psi_B \\ & -\frac{1}{4}\omega_{\mu\nu}\omega^{\mu\nu} + \frac{1}{2}m_\omega^2 \omega_\mu \omega^\mu + \frac{1}{2}(\partial_\mu \sigma \partial^\mu \sigma - m_\sigma^2 \sigma^2) + \sum_\lambda \overline{\psi}_\lambda (i\gamma_\mu \partial^\mu - m_\lambda)\psi_\lambda \\ & -\frac{1}{4}\rho_{\mu\nu}\cdot\rho^{\mu\nu} + \frac{1}{2}m_\rho^2 \rho_\mu \cdot \rho^\mu - \frac{1}{3!}c\sigma^3 - \frac{1}{4!}d\sigma^4 \end{aligned} \tag{1}$$

Where, $\psi_B (B=n,p)$, ψ_λ, σ, ρ and ω are the field operator of baryon (including neutron and proton) and lepton, σ, ω and ρ meson, respectively. $\Gamma_\sigma, \Gamma_\rho$ and Γ_ω are the density-dependent coupling constants, and m_n, m_p, m_σ, m_ρ and m_ω are the mass of neutron, proton, σ, ω and ρ meson, respectively.

From this we can obtain the energy density and pressure of nuclear matter,

$$\begin{aligned} \varepsilon = & \sum_B \frac{\gamma}{(2\pi)^3}\int_0^{k_{FB}} d^3k\sqrt{k^2+(m_B-\Gamma_\sigma\sigma_0)^2} + \frac{1}{2}m_\sigma^2\sigma_0^2 + \frac{1}{2}m_\omega^2\omega_0^2 \\ & + \frac{1}{3!}c\sigma_0^3 + \frac{1}{4!}d\sigma_0^4 + \frac{1}{8}\frac{\Gamma_\rho^2}{m_\rho^2}\rho_3^2 + \sum_\lambda \frac{\gamma}{(2\pi)^3}\int_0^{k_{F\lambda}} d^3k\sqrt{k^2+m_\lambda^2} \end{aligned} \tag{2}$$

$$\begin{aligned} p = & \frac{1}{3}\sum_B \frac{\gamma}{(2\pi)^3}\int_0^{k_{FB}} d^3k \frac{k^2}{\sqrt{k^2+(m_B-\Gamma_\sigma\sigma)^2}} - \frac{1}{2}m_\sigma^2\sigma_0^2 + \frac{1}{2}m_\omega^2\omega_0^2 - \frac{1}{3!}c\sigma_0^3 - \frac{1}{4!}d\sigma_0^4 \\ & + \frac{1}{2}m_\rho^2(\rho^0)_0^2 + \frac{1}{3}\sum_\lambda \frac{\gamma}{(2\pi)^3}\int_0^{k_{F\lambda}} d^3k\frac{k^2}{\sqrt{k^2+m_\lambda^2}} \end{aligned} \tag{3}$$

The binding energy of a nucleon and the incompressibility coefficient are given by

$$E(\rho_B,\delta) = \frac{\varepsilon}{\rho_B} - m_B \tag{4}$$

$$k_0 = 9\rho_{B0}^2 \frac{d^2E(\rho_B,\delta=0)}{d^2\rho_B}|_{\rho_B=\rho_{B0}} \tag{5}$$

Where, ρ_B is number density of baryons, and ρ_{B0} is the saturation density.

The symmetry energy, its slope and curvature at saturation density, are described by

$$S(\rho_B) = \frac{1}{2}\frac{\partial^2 E(\rho_B,\theta)}{\partial{\rho_B}^2}|_{\theta=0} = S(\rho_{B0}) + \frac{1}{3}L\theta + \frac{1}{18}K_{sym}\theta^2,\ \theta = \frac{\rho_B-\rho_{B0}}{\rho_{B0}} \tag{6}$$

$$L = 3\rho_B \frac{\partial S(\rho_B)}{\partial \rho_B}|_{\rho_B=\rho_{B0}} \tag{7}$$

$$K_{sym} = 9\rho_{B0}^2 \frac{\partial^2 S(\rho_B)}{\partial^2 \rho_B}|_{\rho_B=\rho_{B0}} \tag{8}$$

The density-dependent formulas of $\Gamma_{\sigma,\omega,\rho}$ are defined as following, Case I is introduced from references [24], while Case II and Case III are introduced by our work in order to reduce the quantity of coupling constants;

Case I:

$$\Gamma_i(\rho_B) = g_i f_i(x) \tag{9}$$

$$f_i(x) = a_i \frac{1+b_i(x+d_i)^2}{1+c_i(x+d_i)^2}, \; i=\sigma, \; \omega \tag{10}$$

$$\Gamma_\rho(\rho_B) = b_\rho \exp[-a_\rho(x-1)] \tag{11}$$

where $x = \rho_B / \rho_{B0}$, the eight constants in (10) are restricted by $f_i(1)=1$, $f_\sigma^{''}(1) = f_\omega^{''}(1)$ and $f_i^{''}(0)=0$.

Case II:

$$\Gamma_k(\rho_B) = a_k + \log_{b_k}^{\rho_B}, \; k=\sigma, \; \omega, \; \rho \tag{12}$$

Case III:

$$\Gamma_j(\rho_B) = \sqrt{a_j + b_j e^{(-\rho_B/c_j)}}, \; j=\sigma, \; \omega, \; \rho \tag{13}$$

3. NUMERICAL RESULTS

In formulas (10)~(13), the constants a_i, b_i, c_i and d_i ($i(j,k)=\sigma$, ω and ρ), together with c and d in the self-interaction of σ meson are adjusted to fit the binding energy of nuclear matter $E(\rho_{B0}) = -15.75MeV$ and $S(\rho_{B0}) = 31MeV$ at $\rho_{B0} = 0.17 fm^{-3}$. At the same time, the incompressibility coefficient of the EOS should be between 220 and 300 MeV.

The symmetric energy $S(\rho_B)$ in Case I, Case II and Case III, which correspond to the parameters $R\sigma\omega 1$, $R\sigma\omega 5$ and $R\sigma\omega 6$ in table 1, are shown in Figure 1. The values of Γ_ρ and $S(\rho_B)$ at $\rho_B = 0.5 fm^{-3}$ and the values of $S(\rho_B)$, K_{sym} and L at saturation density $\rho_B = 0.17 fm^{-3}$ are shown in Table 1, while the specific values of other parameters are shown in Table 2, several other models are present in Table 2 for comparison. As we can see, greater values of Γ_ρ lead to stiffer $S(\rho_B)$ for $R\sigma\omega 1$ (Case I) in high density region and greater values of K_{sym} and L at saturation density. Similar phenomena happen in other two different density-dependent formulas of $R\sigma\omega 5$ (Case II) and $R\sigma\omega 6$ (Case III).

Table 1: The Data Corresponding to Figure 1

		a_ρ	b_ρ	c_ρ	$\Gamma_\rho(\rho_B=0.5)$	$S(\rho_B=0.5)(MeV)$	$S(\rho_B=0.17)(MeV)$	$L(MeV)$	$K_{sym}(MeV)$
	$R\sigma\omega1-a$	0.04	6.90	/	6.39	77.25	31	82.03	-34.41
$R\sigma\omega1$	$R\sigma\omega1-b$	0.24	6.91	/	4.33	59.42	31	66.30	-102.53
	$R\sigma\omega1-c$	0.74	6.91	/	1.64	46.38	31	26.90	-107.22
$R\sigma\omega2$		0.74	6.94	/	1.65	47.82	31	26.76	-98.24
$R\sigma\omega3$		0.74	7.26	/	1.73	41.43	31	18.64	-121.43
$R\sigma\omega4$		0.74	6.22	/	1.48	55.06	31	42.47	-76.53
	$R\sigma\omega5-a$	5.47	0.24	/	5.96	74.33	31	77.85	-36.43
$R\sigma\omega5$	$R\sigma\omega5-b$	3.84	0.54	/	4.96	65.57	31	67.75	-57.29
	$R\sigma\omega5-c$	0.83	0.74	/	3.13	53.56	31	49.15	-74.31
	$R\sigma\omega6-a$	-64.7	100	-21.2	6.14	87.86	31	93.48	19.56
$R\sigma\omega6$	$R\sigma\omega6-b$	9.5	29	2	5.66	83.30	31	90.95	4.79
	$R\sigma\omega6-c$	11.5	50.0	0.24	5.01	71.67	31	78.40	-40.30
$R\sigma\omega7$		7.56	/	/	7.56	80.09	31	81.3	-26.4

Table 2: The Coupling Constants of Various Models (Include Our Work and Others)

	$K_0(MeV)$	g_σ	g_ω	a_σ	b_σ	c_σ	d_σ	a_ω	b_ω	c_ω	d_ω	c	d
$R\sigma\omega1$	259.97	8.54	9.85	1.25	0.27	0.40	0.91	1.25	0.26	0.39	0.92	100	100
$R\sigma\omega2$	261.10	8.43	9.69	1.25	0.95	1.29	0.51	1.24	1.23	1.65	0.45	100	100
$R\sigma\omega3$	261.60	7.39	8.06	1.27	0.26	0.40	0.91	1.20	0.60	0.80	0.65	100	100
$R\sigma\omega4$	261.08	9.68	11.8	1.30	0.25	0.40	0.91	1.32	0.22	0.37	0.95	0	0
$R\sigma\omega5$	260.14	/	/	7.15	0.39	/	/	8.03	0.50	/	/	100	100
$R\sigma\omega6$	260.30	/	/	82.8	52.7	0.16	/	111.4	90	0.21	/	20	5
$R\sigma\omega7$	261.64	7.11	6.48	/	/	/	/	/	/	/	/	1450	1446
$TW-99$	240.00	10.7	13.3	1.37	0.23	0.41	0.90	1.40	0.17	0.34	0.98	0	0
$DD-ME1$	244.50	10.4	12.9	1.39	0.98	1.53	0.47	1.39	0.85	1.36	0.50	0	0
HA	233.00	9.51	10.4	/	/	/	/	/	/	/	/	7093.9	-255.9
$NL-B1$	280.00	8.76	11.8	/	/	/	/	/	/	/	/	15.029	-100.9

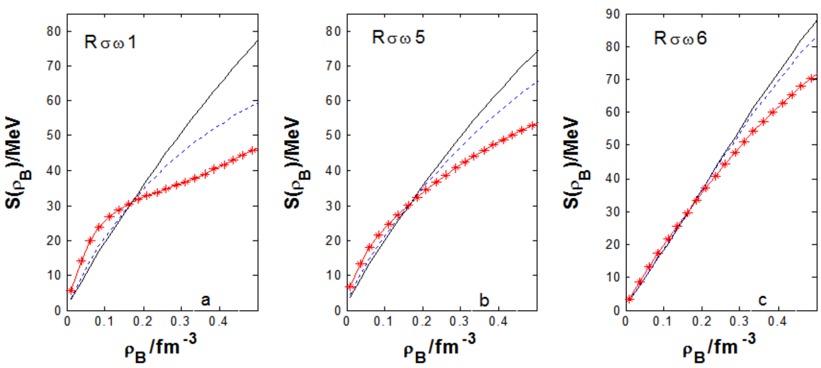

Figure 1: The Influence of Γ_ρ on the Relation between the Nuclear Symmetry Energy $S_{(\rho_B)}$ and ρ_B when $\Gamma_{\sigma,\omega}$, c and d are Fixed. The Solid, Dashed and Asterisk Curves Represent $R\sigma\omega1-a$, $R\sigma\omega1-b$ and $R\sigma\omega1-c$ in Figure 1a, $R\sigma\omega5-a$, $R\sigma\omega5-b$ and $R\sigma\omega5-c$ in Figure 1b, $R\sigma\omega6-a$, $R\sigma\omega6-b$ and $R\sigma\omega6-c$ in Figure 1c, Respectively

In Figure 2a, the value of $S(\rho_B)$ at saturation density being fixed on 31 MeV, seven curves with $K_0 \approx 260MeV$ are shown. The different curves represent the counterpart in Figure 2b, Figure 2c and Figure 2d. As we can see, the symmetry energy in Case I is smaller than the one in other three cases in high density region when K_0 keeps the same value in all cases, and that in non-linear model is the largest. So the density dependence of coupling constants can decrease the symmetry energy in high density region.

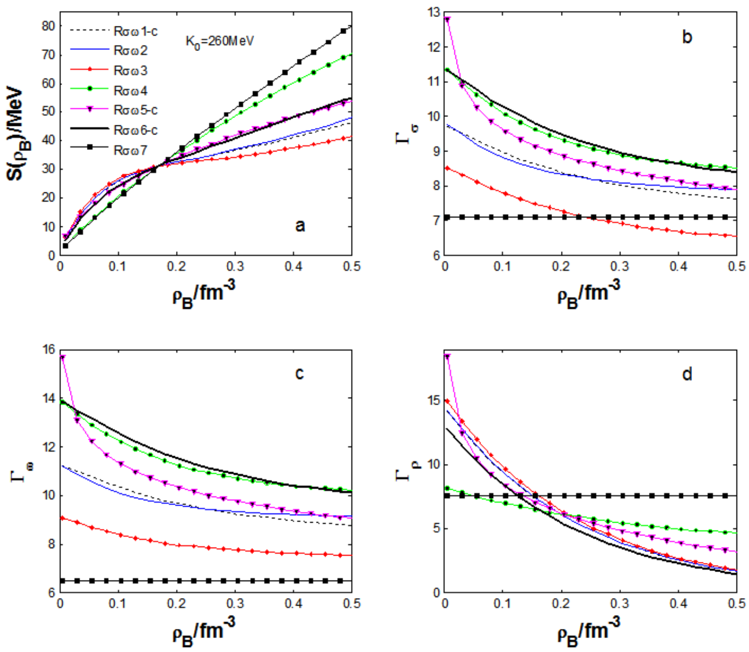

Figure 2: The $S(\rho_B)$ of Nuclear Matter with $K_0 \approx 260MeV$ and Different Values of Other Parameters (Figure 2a), and the Dependence of $\Gamma_{\sigma,\omega,\rho}$ on Nucleon Number Density (Figure 2b, Figure 2c and Figure 2d). The Curves in Figure 2a Represent the Counterparts in Figure 2b, Figure 2c and Figure 2d. The Curves $R\sigma\omega 1-c$ and $R\sigma\omega 2-4$ are Obtained from Case I in Table 1 and 2, while $R\sigma\omega 5-c$, $R\sigma\omega 6-c$ and $R\sigma\omega 7$ are Gained from Case II, Case III and Non-Linear Model, Respectively

In Figure 3, we depict the correlations between L and K_{sym} at saturation density with K_0 restricted between 220 and 300 MeV, the distribution range of L and K_{sym} are different in different density-dependent formulas at the same density. An approximate linear correlation ($K_{sym} = 2.63L - 176.21$) exists in the range of $10 < L < 60MeV$ and $-140 < K_{sym} < -40MeV$ for Case I, but it disperses when $L > 60MeV$, while $70 < L < 90MeV$ and $-80 < K_{sym} < 0MeV$ for Case II, $40 < L < 80MeV$ and $-100 < K_{sym} < -60MeV$ for Case III, $80 < L < 90MeV$ and $-30 < K_{sym} < 0MeV$ for non-linear model. The values of L in all models are shown in Figure 4. As we can see, the range of the values of L obtained in this work is consistent with those obtained from other analyses.

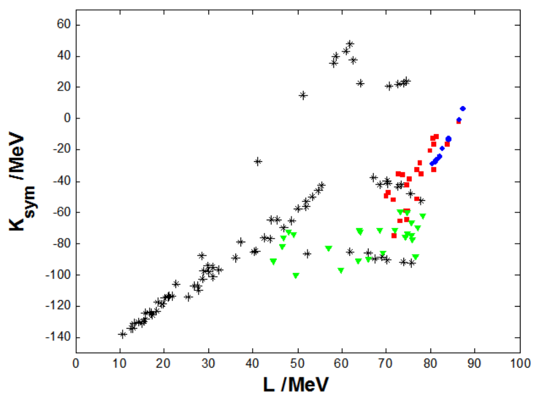

Figure 3: the Correlations between L and K_{sym} Calculated by Different Parameters at Saturation Density with K_0 Restricted between 220 and 300 MeV. The Asterisks, Squares, Triangles and Circles Represent the Values of L and K_{sym} in Case I, Case II, Case III and Non-Linear Model, Respectively

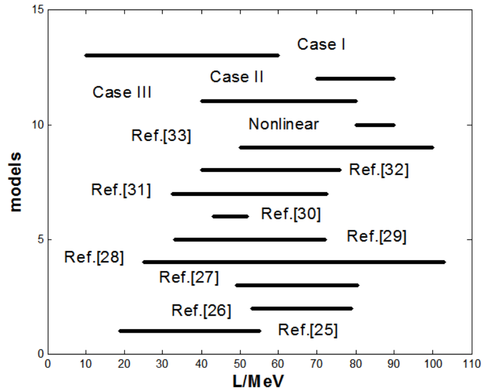

Figure 4: The Values of L from All Models

Similar to the symmetry energy as a function of nucleon density in Figure 1, we will study the density dependence of correlation between L and K_{sym}. In Figure 5, the correlation between L and K_{sym} in various cases at $\rho_B = 0.5\rho_0$, ρ_0, $2\rho_0$ and $3\rho_0$ are shown, respectively. In Case I, the scatter plot which is obtained by changing parameters moves to the left when the density increases. At the same time, the range of L is up to its maximum around the saturation density while the one of K_{sym} keeps minimum as $\rho_B \geq \rho_0$. On the other hand, L and K_{sym} are positively correlated when ρ_B is about less than ρ_0, and they become to be negatively correlated when ρ_B is greater than ρ_0. In the last three cases, similar phenomena happen. Different from Case I, the variation of L and K_{sym} decrease obviously. It means that L and K_{sym} vary a little when the parameters are changed in these three cases and they are the smallest in non-linear model. In conclusion, the density dependence of coupling constants can make L and K_{sym} sensitive to the changing of parameters, and Case I is most likely to reproduce the experimental results for it being the most sensitive.

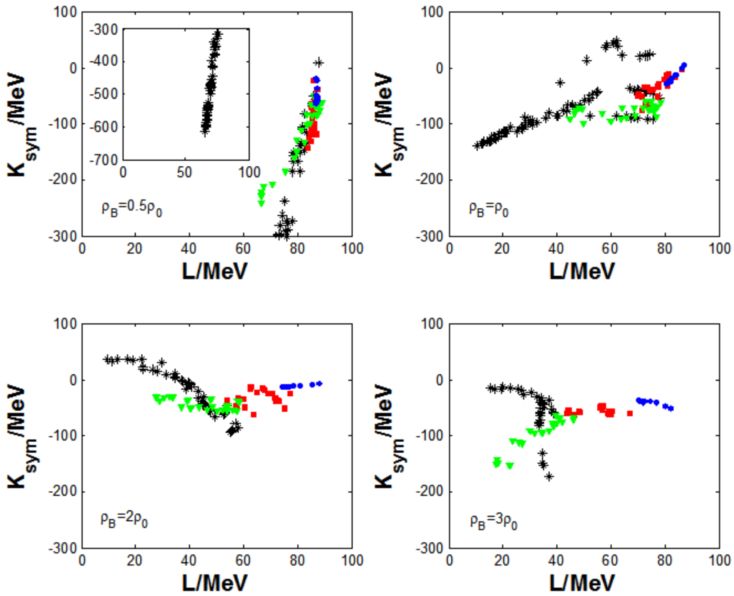

Figure 5: The Same as Figure 3 at 0.5, 1, 2 and 3 Times Saturation Density for Comparison

4. CONCLUSIONS

In the mean field approximation of nonlinear relativistic $\sigma-\omega-\rho$ model, we study the influence of density-dependent coupling constants on binding energy of a nucleon and $S(\rho_B)$ of infinite symmetric nuclear matter. We found that greater values of Γ_ρ lead to greater K_{sym} and L when $\Gamma_{\sigma,\omega}$, c and d are fixed and indicate stiffer $S(\rho_B)$ in high density region. In addition, the density dependence of coupling constants can not only decrease the symmetry energy in higher density region but also make L and K_{sym} sensitive to the changing of parameters and Case I is most likely to reproduce the experimental results for its highest sensitivity.

5. REFERENCES

1. *Feng Z Q. Constraining the high-density behavior of the nuclear equation of state from strangeness production in heavy-ion collisions[J]. Physical Review C, 2011, 83(6): 067604.*
2. *Kumar S, Ma Y G, Zhang G Q, et al. Probing the density dependence of symmetry energy via multifragmentation at sub-saturation densities[J]. Physical Review C, 2011, 84(4):1291-1293.*
3. *Ma C W, Wang F, Ma Y G, et al. Isobaric yield ratios in heavy-ion reactions, and symmetry energy of neutron-rich nuclei at intermediate energies[J]. Physical Review C, 2011, 83(6):2795-2805.*
4. *Steiner A W, Prakash M, Lattimer J M, et al. "Isospin Asymmetry in Nuclei and Neutron Stars," Physiological Reports, 2005, 411(6): 325-375.*
5. *Chen L W, Ko C M, Li B A. Determination of the stiffness of the nuclear symmetry energy from isospin diffusion[J]. Physical Review Letters, 2005, 94(3):032701.*
6. *Shetty D V, Yennello S J, Souliotis G A. Density dependence of the symmetry energy and the equation of state of isospin asymmetric nuclear matter[J]. Physical Review C, 2007, 75(3): 034602.*
7. *Tsang M B, Zhang Y, Danielewicz P, et al. Constraints on the density dependence of the symmetry energy[J]. Physical review letters, 2009, 102(12): 122701.*
8. *Wang Y, Guo C, Li Q, et al. 3H/3He ratio as a probe of the nuclear symmetry energy at sub-saturation densities[J]. The European Physical Journal A, 2015, 51(3): 37.*
9. *Loan D T, Loc B M, Khoa D T. Extended Hartree-Fock study of the single-particle potential: The nuclear symmetry energy, nucleon effective mass, and folding model of the nucleon optical potential[J]. Physical Review C, 2015, 92(3): 034304.*
10. *Zhao Q, Sun B Y, Long W H. Kinetic and potential parts of nuclear symmetry energy: the role of Fock terms[J]. Journal of Physics G: Nuclear and Particle Physics, 2015, 42(9): 095101.*
11. *Kaur M, Gautam S, Puri R K. Fragmentation in isotopic and isobaric systems as probe of density dependence of nuclear symmetry energy[J]. Nuclear Physics A, 2016, 955: 133-144.*
12. *Ou L, Xiao Z, Yi H, et al. Dynamic isovector reorientation of deuteron as a probe to nuclear symmetry energy[J]. Physical review letters, 2015, 115(21): 212501.*

13. *Mishra R N, Sahoo H S, Panda P K, et al. Nuclear symmetry energy in a modified quark-meson coupling model[J]. Physical Review C, 2015, 92(4): 045203.*
14. *Mondal C, Agrawal B K, De J N. Constraining the symmetry energy content of nuclear matter from nuclear masses: A covariance analysis[J]. Physical Review C, 2015, 92(2): 024302.*
15. *Mondal C, Agrawal B K, De J N, et al. Sensitivity of elements of the symmetry energy of nuclear matter to the properties of neutron-rich systems[J]. Physical Review C, 2016, 93(4): 044328.*
16. *Inakura T, Nakada H. Constraining the slope parameter of the symmetry energy from nuclear structure[J]. Physical Review C, 2015, 92(6): 064302.*
17. *López J A, Porras S T. Symmetry energy in the liquid–gas mixture[J]. Nuclear Physics A, 2017, 957: 312-320.*
18. *Bao S S, Shen H. Effects of finite size and symmetry energy on the phase transition of stellar matter at subnuclear densities[J]. Physical Review C, 2016, 93(2): 025807.*
19. *Mondal C, Agrawal B K, Centelles M, et al. Model dependence of the neutron-skin thickness on the symmetry energy[J]. Physical Review C, 2016, 93(6): 064303.*
20. *Jiang H, Wang N, Chen L W, et al. Model dependence of the I 4 term in the symmetry energy for finite nuclei[J]. Physical Review C, 2015, 91(5): 054302.*
21. *Roca-Maza X, Brenna M, Colò G, et al. Electric dipole polarizability in 208 Pb: Insights from the droplet model[J]. Physical Review C, 2013, 88(2): 024316.*
22. *Carbone A, Colò G, Bracco A, et al. Constraints on the symmetry energy and neutron skins from pygmy resonances in Ni 68 and Sn 132[J]. Physical Review C, 2010, 81(4): 041301.*
23. *Alonso D, Sammarruca F. Microscopic calculations in asymmetric nuclear matter[J]. Physical Review C, 2003, 67(5): 054301.*
24. *Typel S, Wolter H H. Relativistic mean field calculations with density-dependent meson-nucleon coupling[J]. Nuclear Physics A, 2000, 656(3-4):331-364.*
25. *Roca-Maza X, Brenna M, Agrawal B K, et al. Giant quadrupole resonances in 208 Pb, the nuclear symmetry energy, and the neutron skin thickness[J]. Physical Review C, 2013, 87(3): 034301.*
26. *Liu M, Wang N, Li Z X, et al. Nuclear symmetry energy at subnormal densities from measured nuclear masses[J]. Physical Review C, 2010, 82(6): 064306.*
27. *Warda M, Vinas X, Roca-Maza X, et al. Neutron skin thickness in the droplet model with surface width dependence: Indications of softness of the nuclear symmetry energy[J]. Physical Review C, 2009, 80(2): 024316.*
28. *Roca-Maza X, Centelles M, Vinas X, et al. Neutron skin of Pb 208, nuclear symmetry energy, and the parity radius experiment[J]. Physical review letters, 2011, 106(25): 252501.*
29. *Lattimer J M, Steiner A W. Constraints on the symmetry energy using the mass-radius relation of neutron stars[J]. European Physical Journal A, 2014, 50(2):1-24.*

30. *Steiner A W, Gandolfi S. Connecting neutron star observations to three-body forces in neutron matter and to the nuclear symmetry energy[J]. Physical review letters, 2012, 108(8): 081102.*

31. *Chen L W. Nuclear matter symmetry energy and the symmetry energy coefficient in the mass formula[J]. Physical Review C, 2011, 83(4): 044308.*

32. *Chen L W, Ko C M, Li B A, et al. Density slope of the nuclear symmetry energy from the neutron skin thickness of heavy nuclei[J]. Physical Review C, 2010, 82(2): 024321.*

33. *Centelles M, Roca-Maza X, Vinas X, et al. Nuclear symmetry energy probed by neutron skin thickness of nuclei[J]. Physical review letters, 2009, 102(12): 122502.*